

Tunneling in the $\text{H}_2\text{S} + \text{O}(^3\text{P}) \rightarrow \text{HS} + \text{OH}$ reaction: A theoretical study

Keiichi Yokoyama and Toshiyuki Takayanagi

Citation: *The Journal of Chemical Physics* **104**, 1953 (1996); doi: 10.1063/1.470949

View online: <http://dx.doi.org/10.1063/1.470949>

View Table of Contents: <http://scitation.aip.org/content/aip/journal/jcp/104/5?ver=pdfcov>

Published by the AIP Publishing

Articles you may be interested in

An ab initio analytical potential energy surface for the $\text{O}(^3\text{P}) + \text{CS}(^1\Sigma^+) \rightarrow \text{CO}(^1\Sigma^+) + \text{S}(^3\text{P})$ reaction useful for kinetic and dynamical studies

J. Chem. Phys. **105**, 10999 (1996); 10.1063/1.472899

A global H_2O potential energy surface for the reaction $\text{O}(^1\text{D}) + \text{H}_2 \rightarrow \text{OH} + \text{H}$

J. Chem. Phys. **105**, 10472 (1996); 10.1063/1.472977

An interpolated unrestricted Hartree–Fock potential energy surface for the $\text{OH} + \text{H}_2 \rightarrow \text{H}_2\text{O} + \text{H}$ reaction

J. Chem. Phys. **104**, 4600 (1996); 10.1063/1.471207

An analytical representation of the lowest potential energy surface for the reaction $\text{O}(^3\text{P}) + \text{HCl}(^1\Sigma^+) \rightarrow \text{OH}(^2\Pi) + \text{Cl}(^2\text{P})$

J. Chem. Phys. **95**, 6421 (1991); 10.1063/1.461562

Ab initio transition state theory calculations of the reaction rate for $\text{OH} + \text{CH}_4 \rightarrow \text{H}_2\text{O} + \text{CH}_3$

J. Chem. Phys. **93**, 1761 (1990); 10.1063/1.459103



NEW Special Topic Sections

NOW ONLINE
Lithium Niobate Properties and Applications:
Reviews of Emerging Trends

AIP Applied Physics Reviews

Tunneling in the $\text{H}_2\text{S} + \text{O}(^3P) \rightarrow \text{HS} + \text{OH}$ reaction: A theoretical study

Keiichi Yokoyama and Toshiyuki Takayanagi

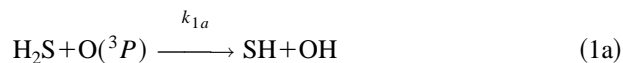
Advanced Science Research Center, Japan Atomic Energy Research Institute, Tokai-mura, Ibaraki, 319-11 Japan

(Received 31 May 1995; accepted 25 October 1995)

Title reaction has been investigated by a quantum mechanical reactive scattering method. A potential energy surface has been constructed on the basis of *ab initio* calculations at the MP2(fc)/6-311G(3df,3pd) level of theory. The reaction probabilities have been calculated under an assumption of a collinear atom-diatom collision. It has been found that $\text{OH}(v=1)$ is mainly produced in the reaction at room temperature. The rate constants evaluated from the reaction probabilities were 2 orders of magnitude higher than those calculated by the transition-state theory, implying that quantum mechanical tunneling plays an important role in this reaction even at room temperature. © 1996 American Institute of Physics. [S0021-9606(96)01505-0]

I. INTRODUCTION

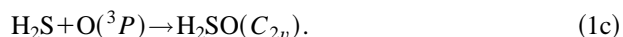
The reaction of hydrogen sulfide with the oxygen atom in its ground electronic state is thought to proceed by the following scheme:



Reaction (1a) is a hydrogen abstraction reaction. Singleton and co-workers reported that the branching ratio, $k_{1b}/(k_{1a} + k_{1b})$, is less than 0.2 at room temperature from their product analysis after mercury-photosensitization.¹ Reaction (1b) is a hydrogen substitution. Production of the HSO radical was confirmed in crossed molecular beams experiments by Davidson and co-workers^{2,3} and Balucani and co-workers.⁴ They have suggested that reaction (1b) proceeds *via* direct mechanism without formation of an intermediate complex H_2SO . Threshold energy of reaction (1b) was measured to be $14 \pm 2 \text{ kJ mol}^{-1}$.² This value is close to the activation energy of reaction (1) measured to be 16 kJ mol^{-1} (Ref. 5), $13.8 \pm 0.4 \text{ kJ mol}^{-1}$ (Ref. 6), and $18.0 \pm 1.7 \text{ kJ mol}^{-1}$ (Ref. 7) over the temperature range of 250–500 K. Reaction (1b), then, competes with reaction (1a). Recently Tsuchiya and co-workers have determined the branching ratio $k_{1b}/(k_{1a} + k_{1b})$ to be 0.2 ± 0.1 in the temperature range from 1520 to 1820 K.⁸ They have also measured the activation energy of reaction (1) as $32 \pm 4 \text{ kJ mol}^{-1}$ at the high temperature. This result indicates that the activation energy obtained at lower temperatures is different from that obtained at higher temperatures. Therefore, the Arrhenius plot of $k_1 (= k_{1a} + k_{1b})$ is found to deviate from a linear relation. This suggests that quantum mechanical tunneling plays an important role even at room temperatures.

Takane and Fueno have theoretically studied the mechanism of reactions (1a) and (1b) by a multireference single- and double-excitation configuration interaction method.⁹ They have found that reaction (1b) proceeds *via* direct substitution mechanism supporting the conclusion obtained from the experimental result by Balucani and co-workers. Zhu and

co-workers pointed out possibility of an out-of-plane approach of $\text{O}(^3P)$ to form a planar intermediate H_2SO with the MP2/6-311G(*d,p*) level.¹⁰



Goumri and co-workers have recently calculated the barrier heights for reactions (1a), (1b), and (1c) with the G2 theory¹¹ and have found that the respective transition states, $\text{TS}_{1a}(^3A')$, TS_{1b} , and TS_{1c} , have barrier heights of 23.4, 27.9, and 116.1 kJ mol^{-1} , respectively. They have also calculated the temperature dependence of the rate constants, k_{1a} , by a simple transition-state theory including the Wigner correction¹² for the tunneling effect. Although their results agree quite well with the experimental rate constants, the tunneling correction is not accurate as they mentioned. In the present paper, we treat tunneling with more sophisticated method.

Since reaction (1a) predominantly occurs at room temperature, we calculate only the temperature dependence of k_{1a} to reproduce the measured temperature dependence of the overall rate constant k_1 . To calculate k_{1a} including the tunneling effect, we carry out quantum mechanical reactive scattering calculations. The aim is the rigorous solution of time-independent Schrödinger equation of nuclear motion within the Born–Oppenheimer approximation. The computational method has been developed so far^{13–15} for three-atom reactions. For four-atom reactions, new approximations for numerical computation are being developed recently.^{16–25} In this paper, we treat reaction (1a) as a simple collinear atom-diatom reaction.

II. COMPUTATIONAL METHOD

Ab initio molecular orbital calculations are employed to determine which level is accurate enough to construct the potential energy surface (PES) for reaction (1a). Molecular structures of major points including transition states (TS's) and fragments are calculated by the unrestricted Hartree–Fock (HF) energy gradient method with the 6-31G(*d,p*) basis set. Vibrational analyses of those points are carried out by the same method. Single point energies are obtained at the

QCISD(T)/6-31G(*d,p*) + Ryd and MP2(fc)/6-311G(3*df*,3*pd*) levels of theory, where “Ryd” indicates an *s* function with an exponent $\zeta=0.023$ on the S atom.²⁶ All the *ab initio* calculations are performed by GAUSSIAN 90.²⁷

The potential energy surface (PES) of reaction (1a) consists of two-dimensional cubic spline functions fitted to the MP2(fc)/6-311G(3*df*,3*pd*) energies. We choose the dissociating S–H bond length, R_{SH} , and forming O–H bond length, R_{HO} , as variables. The angle $\angle\text{SHO}$ is fixed at 180° , that is a “collinear collision” if the spectator H atom is ignored. We designate the spectator H atom as H' later in this paper. The other internal coordinates, the bend angle $\angle\text{H}'\text{SH}$ and the spectator H' –S bond length, are fixed at the TS geometries. Although there are two states $^3A'$ and $^3A''$ which should degenerate if reaction (1a) were considered as a true atom-diatom reaction, we calculate only the $^3A'$ surface in detail and check that the $^3A''$ surface has almost the same barrier height and TS structure. The bond lengths R_{SH} and R_{HO} are varied in the ranges 0.8–3.0 Å and 0.6–2.6 Å, respectively. As a result, potential energies of 110 geometries are used for constructing the PES.

The scattering calculations are performed by using hyperspherical coordinates.²⁸ A Hamiltonian for collinear atom-diatom collisions is written as

$$H(\rho, \theta) = -\frac{\hbar^2}{2\mu} \frac{\partial^2}{\partial \rho^2} + \frac{3\hbar^2}{8\mu\rho^2} + H_\theta(\rho, \theta), \quad (2)$$

$$H_\theta(\rho, \theta) = -\frac{\hbar^2}{2\mu\rho^2} \frac{\partial^2}{\partial \theta^2} + V(\rho, \theta),$$

where

$$\mu = \left(\frac{m_{\text{HS}}m_{\text{H}}m_{\text{O}}}{m_{\text{HS}} + m_{\text{H}} + m_{\text{O}}} \right)^{1/2},$$

$$\rho = \left(\frac{m_{\text{HS}}(m_{\text{H}} + m_{\text{O}})}{m_{\text{HS}} + m_{\text{H}} + m_{\text{O}}} \frac{R_{\text{SH}}^2}{\mu} + \frac{m_{\text{H}}m_{\text{O}}}{m_{\text{H}} + m_{\text{O}}} \frac{R_{\text{HO}}^2}{\mu} \right)^{1/2},$$

$$\theta = \arctan \left[\left(\frac{m_{\text{H}}m_{\text{O}}(m_{\text{HS}} + m_{\text{H}} + m_{\text{O}})}{m_{\text{HS}}(m_{\text{H}} + m_{\text{O}})^2} \frac{R_{\text{HO}}^2}{R_{\text{SH}}^2} \right)^{1/2} \right]. \quad (3)$$

First, H_θ is diagonalized for a given value of $\rho = \rho_i$ to obtain adiabatic levels. Then the overlap integrals between these states are calculated and the close-coupling equations are solved by the *R*-matrix propagation method²⁹ to determine the *S* matrix. The reaction probability of going from the state ν to the state ν' with total energy E is calculated from the *S* matrix as

$$P_{\nu \rightarrow \nu'}(E) = |S_{\nu\nu'}(E)|^2, \quad (4)$$

where ν is the vibrational quantum number of the S–H stretching and ν' the O–H stretching.

The cross section from the initial state ν to the final state ν' is calculated by using the reaction probability with the *J*-shift approximation.³⁰

$$\sigma_{\nu \rightarrow \nu'}(E_T) = \frac{\pi \hbar^2}{2\mu E_T} \sum_J (2J+1) P_{\nu \rightarrow \nu'}^J(E_T), \quad (5)$$

$$P_{\nu \rightarrow \nu'}^J(E_T) = P_{\nu \rightarrow \nu'}(E_T + E_\nu - E_b - E_c),$$

where E_T is the collisional energy, E_ν the asymptotic energy of the initial state ν , E_b the zero-point vibrational energy for in-plane and out-of-plane SHO bending motions at the TS, and E_c the centrifugal energy written by

$$E_c = \frac{J(J+1)}{2\mu R^\ddagger{}^2}, \quad R^\ddagger: \text{constant}, \quad (6)$$

where J is the total angular momentum. If the cross section summed over final states

$$\sigma_\nu(E_T) = \sum_{\nu'} \sigma_{\nu \rightarrow \nu'}(E_T) \quad (7)$$

is independent of the rotational states of H_2S and products, the rate constant of the initial state ν is given by

$$k_\nu(T) = \left(\frac{8}{\pi\mu} \right)^{1/2} (k_B T)^{-3/2} \int_0^\infty \sigma_\nu(E_T) E_T e^{E_T/k_B T} dE_T. \quad (8)$$

Then the overall rate constant is calculated by

$$k(T) = f_e(T) \sum_\nu f_\nu(T) k_\nu(T), \quad (9)$$

where $f_e(T)$ is the probability of finding a $\text{O}(^3P_J)$ atom in six spin-orbit states correlating to the $^3A'$ or $^3A''$ abstraction surfaces. $f_\nu(T)$ is the probability of finding an H_2S molecule in the vibrational state ν .

III. RESULTS

Theoretical heats of reactions ΔH_r for five channels of reaction (1) are listed in Table I together with respective experimental values. Apparently, the MP2(fc)/6-311G(3*df*,3*pd*) energies well agree with the experimental. Note that the large basis set gives good results even with the MP2 level of theory, while the smaller one, 6-31G(*d,p*) + Ryd, does not lead quantitative results even with the QCISD(T) or MRDCI (Ref. 9) level. We, therefore, adopt the MP2(fc)/6-311G(3*df*,3*pd*) energies to construct the PES.

Structures of two TS's for reactions (1a) are shown in Fig. 1 with notations of $\text{TS}_{1a}(^3A')$ and $\text{TS}_{1a}(^3A'')$, respectively. Both structures are planar. These transition states have almost the same structure, which has a nearly-collinear configuration along the S–H–O atoms, i.e., the angle $\angle\text{SHO}$ is 175.1° for $^3A'$ and 170.6° for $^3A''$. The angle $\angle\text{H}'\text{SH}$ and the spectator bond length $R(\text{H}'\text{S})$ are close to those of the H_2S molecule. Therefore, the model of collinear atom-diatom collision that we chose to describe reaction (1a) is supposed to be adequate.

Threshold energies ΔH_0^\ddagger for TS_{1a} and TS_{1b} are also listed in Table I. These values are the barrier heights including vibrational zero-point energies. Clearly, the A' and A'' states nearly degenerate at TS_{1a} and then, both channels can comparably occur. The threshold energy for reaction (1b) is

TABLE I. Calculated zero-point vibrational energies, heats of reactions, and experimental heats of reactions in units of kJ mol^{-1} .

		ΔH_0				
Structure	ZPE	MP2/ <i>B1</i> ^a	QCISD(T)/ <i>B1</i> ^a	MP2/ <i>B2</i> ^b	Expt. ^c	
	H ₂ S+O(³ <i>P</i>)	43.0	(0.701 41) ^d	(0.731 81) ^d	(0.847 19) ^d	
1 <i>a</i>	SH+OH	41.0	−45.5	−33.4	−49.7	−49.4
1 <i>b</i>	HSO+H	29.0	48.3	25.7	−19.9	−17
1 <i>c</i>	H ₂ SO(³ <i>B</i> ₁)	35.8	114.4	93.5	1.3	
1 <i>d</i>	SO+H ₂	36.0	−181.6	−178.2	−235.5	−223.4
1 <i>e</i>	SH+O+H	17.0	340.5	345.1	366.4	366
	TS _{1<i>a</i>} (³ <i>A</i> [′])	32.0	79.8	40.9	36.9	13.8–18.0 ^e
			(391,473,482,1096,2887,3150 <i>i</i>) ^g			
	TS _{1<i>a</i>} (³ <i>A</i> [″])	45.4	241.7	58.9	34.6	
			(298,557,1260,2592,2897,712 <i>i</i>) ^g			
	TS _{1<i>b</i>} (³ <i>A</i> [″])	34.0	116.9	67.6	38.7	14±2 ^f
			(291,569,672,1216,2901,1092 <i>i</i>) ^g			
	TS _{1<i>c</i>}	38.6	173.6	140.5	98.6	
			(440,701,1051,2083,2180,802 <i>i</i>) ^h			

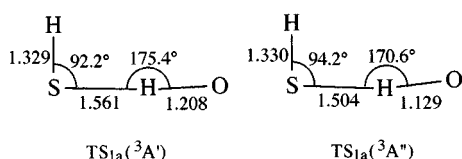
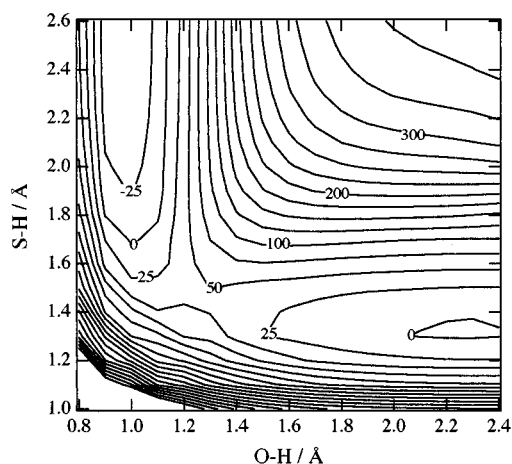
^a6-31G(*d,p*) + Ryd.^b6-311G(3*df*,3*pd*).^cReference 3 and references therein.^dTotal energy +473 in atomic units.^eActivation energies measured for k_1 .^fThreshold energy for reaction (1b) measured in molecular beam experiments.^gNormal mode frequencies (cm^{-1}) calculated by the HF/6-31G(*d,p*) method.^hNormal mode frequencies (cm^{-1}) calculated by the MP2(fu)/6-311G(*d,p*) method.

not so high that reaction (1b) can compete with reaction (1a). These relations are consistent with the experimental observations that both channels were observed. On the other hand, the absolute values of the theoretical threshold energies are higher by $\sim 20 \text{ kJ mol}^{-1}$ than the respective experimental activation energies at room temperature. The discrepancy seems too large even if we consider that threshold energy is not equal to activation energy.

Figure 2 shows a contour plot of the PES of the $^3A'$ state for reaction (1a). OH vibrational frequency 3691 cm^{-1} calculated from the PES is compared quite well to the experimental frequency 3735 cm^{-1} . The SH local stretching was calculated to be 2643 cm^{-1} , which is close to the asymmetric stretching 2627 cm^{-1} and symmetric 2615 cm^{-1} of H_2S . The saddle point is located at a slightly reactant-side region on the PES, that is, reaction (1a) has an “early” transition state. The barrier height is obtained to be 49 kJ mol^{-1} from the PES.

The vibrational adiabatic levels calculated as a function of hyperradius ρ are shown in Fig. 3. The total energy E in the ordinate is measured from the bottom of the reactant

valley. Since most of the reactants are populated in the ground vibrational state at room temperature, only the lowest three states in this figure are required to describe the room-temperature reaction, i.e., one initial state $\text{H}_2\text{S}(v=0)$ and two final states $\text{OH}(v'=0 \text{ and } 1)$. In particular, the $\text{OH}(1)$ state almost degenerates with the $\text{H}_2\text{S}(0)$ state. This may cause significant interaction between the initial state and the final one. As shown in Fig. 4, the probability of the reaction $\text{H}_2\text{S}(0) + \text{O} \rightarrow \text{OH}(1) + \text{HS}$, designated by P_{01} , is, in fact, much greater than P_{00} over the collisional energy range

FIG. 1. Transition-state structures calculated by HF/6-31G(*d,p*) method. Bond lengths are in Å and bond angle in degrees.FIG. 2. Contour plot of the potential energy surface for reaction (1a) constructed by the MP2(fc)/6-311G(3*df*,3*pd*) energies. Inserted numbers are relative potential energies in kJ mol^{-1} measured from the bottom of the reactant valley (right hand side, bottom).

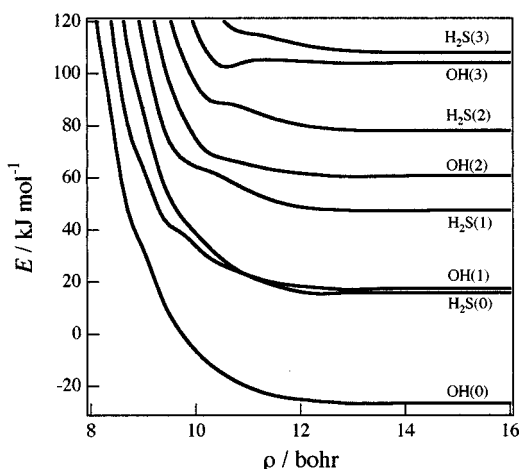


FIG. 3. Vibrational adiabatic curves as a function of hyperspherical radius ρ . "OH(n)" means a final state for $\text{OH}(v'=n) + \text{SH}$ and " $\text{H}_2\text{S}(m)$ " an initial state for $\text{H}_2\text{S}(v=m) + \text{O}$. The total energy E in the ordinate is measured from the bottom of the reactant valley.

0–100 kJ mol^{-1} , implying strong interaction between the initial and the final states. Therefore we take only P_{01} into account in the calculation of the rate constant.

The reaction probability P_{01} rises around a collisional energy of $E_T = 20 \text{ kJ mol}^{-1}$, which is much lower than the *ab initio* threshold energy $\Delta H_0^\ddagger = 36.9 \text{ kJ mol}^{-1}$ for $\text{TS}_{1a}(^3A')$. We think that the low appearance energy can be partly attributed to tunneling from the $\text{SH}(0)$ state to the $\text{OH}(1)$ state.

The rate constant of reaction (1a), k_{1a} , was calculated from P_{01} , using $R^\ddagger = 5.2 \text{ bohr}$ in Eq. (6). Figure 5 shows the temperature dependence of k_{1a} together with experimental values of k_1 . Unfortunately, the calculated rate constant is 1 order of magnitude lower than the experimental rate constant at room temperature. We suppose that this discrepancy may stem from the large barrier height of the PES used in the

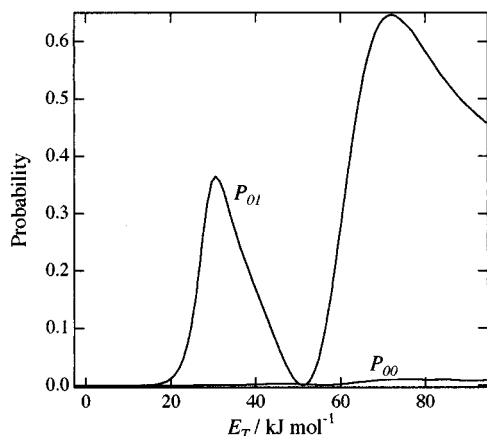


FIG. 4. Reaction probabilities of state-to-state reactions as a function of collision energy. P_{01} means the reaction probability of the reaction $\text{H}_2\text{S}(0) + \text{O} \rightarrow \text{OH}(1) + \text{SH}$.

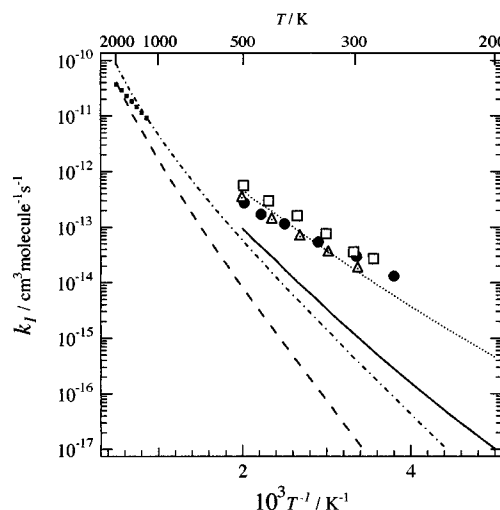


FIG. 5. Comparison of the temperature dependence of k_{1a} obtained from the scattering calculations (solid line), transition-state theory calculation (dashed line), scattering calculations using the scaled potential energy surface (dotted line), and transition-state theory calculations using the scaled barrier height (dotted-dashed line) with k_1 measured experimentally by Singleton and co-workers (Δ), Whytock and co-workers (\bullet), Slagle and co-workers (\square), and Tsuchiya and co-workers (\blacksquare).

scattering calculations because the barrier height is calculated to be 11 kJ mol^{-1} higher than that of the G2 theory.¹¹

Figure 5 also shows the temperature dependence of k_{1a} calculated from the transition-state theory (TST) by using the HF molecular structures and vibrational frequencies without tunneling correction. Comparing these two theoretical curves, we can conclude that the tunneling accelerates reaction (1a) by about 2 orders of magnitude at room temperature.

IV. DISCUSSION

Although the MP2/6-311G(3df,3pd) level gives good results for the heat of reaction, this does not guarantee that the theory would be effective even in the saddle point region. For example, spin contamination generally becomes significant in an open-shell electronic state at intermediate bond length far from equilibrium value. In such a case spin projection might be needed to the unrestricted MP2 theory.^{31,32} However, in this case the eigenvalue of the operator s^2 for $\text{TS}_{1a}(^3A')$ was calculated to be 2.078, which was close to the true eigenvalue 2.0 for pure triplet eigenstate. Then we do not involve the spin projection to construct the PES. Nevertheless, the calculated barrier height is considerably larger than the G2 energy. This indicates that the MP2 theory is insufficient to treat electronic correlation energy in the saddle point region.

Since the *ab initio* barrier height used here seems too large, we modify the PES so as to give a rate constant closer to the observed. We carry out the modification by subtracting a two-dimensional Gaussian function from the *ab initio* potential energies V . The modified potential energies V' are calculated by

$$V' = V - A \exp[-\alpha_1(R_{\text{HO}} - R_{\text{HO}}^\ddagger)^2 - \alpha_2(R_{\text{SH}} - R_{\text{SH}}^\ddagger)^2],$$

where R_{HO}^\ddagger ($=2.432 \text{ \AA}$) and R_{SH}^\ddagger ($=2.753 \text{ \AA}$) are the bond lengths for the saddle point and A , α_1 , and α_2 are fitting parameters. It has been found that satisfying temperature dependence for k_{1a} is obtained from the scattering calculation with $A=8.7 \text{ kJ mol}^{-1}$ and $\alpha_1=\alpha_2=0.5 \text{ \AA}^{-2}$. The temperature dependence and the absolute values of the rate constant are quite well reproduced as shown in Fig. 5. The TST calculation using lowered barrier height gives very low values and implies that tunneling is still important on the modified PES.

We did not examine the tunneling effect of reaction (1b), because reaction (1b) is supposed to be a minor channel in the overall reaction. Tsuchiya and co-workers calculated the temperature dependence of the branching ratio, k_{1b}/k_1 , with the Rice–Ramsperger–Kassel–Marcus (RRKM) theory.⁸ According to their estimation, the branching ratio is about 0.1 at room temperature. In addition, tunneling itself may be less important in reaction (1b) than in reaction (1a). The mass-weighted PES for reaction (1a) possesses a skew angle of 17° while for reaction (1b) the angle is 84° . This indicates that the PES for reaction (1b) has a thick ridge in the saddle point region in comparison with that for reaction (1a). So tunneling should be less important in reaction (1b).

We explicitly treated the SH and OH stretching vibration in the scattering calculation. There are some other internal degrees of freedom, the spectator H'S stretching, H_2S bending, H_2S rotation and products rotations. The spectator H'S bond length is invariant throughout the reaction; i.e., $1.327 \text{ (H}_2\text{S)}$, 1.330 (TS) , and 1.331 \AA (HS) and, thus, the mode does not affect the reaction dynamics. Excitation of the bending motion of H_2S can be ignored at room temperature because the frequency of 1182 cm^{-1} is too large for the excited bend states to be populated. The product rotation is expected to be cold from analogy with reactions $\text{H}_2\text{O} + \text{Cl} \rightarrow \text{OH} + \text{HCl}$ (Ref. 16) and $\text{H}_2\text{O} + \text{H} \rightarrow \text{OH} + \text{H}_2$ (Ref. 17). We, therefore, pay attention to only the reactant rotation. Rotational effects of reactants were studied with the rotating bond approximation model by Nyman and Clary in the reaction $\text{H}_2\text{O} + \text{Cl} \rightarrow \text{OH} + \text{HCl}$. According to their calculation, the cross section does not change largely with the reactant rotation, although the most probable quantum number of final rotational states increases as the initial rotational state quantum number increases. Thus we assumed that the cross section were independent of the H_2S rotation in the rate constant calculations.

P_{01} exhibits a sharp maximum like a “resonance” at a collisional energy of 31 kJ mol^{-1} in Fig. 4. The “resonance” structure is known in reactive scattering calculations for some abstraction reactions.^{33,34} Their origin is thought to be unstable periodic orbits around the saddle point region in a classical sense. An antisymmetric stretching mode in the unstable periodic orbits mainly consists of the linear vibration of the H atom along the S–H–O line with little displacement of the S and O atoms, and thus, may enhance the tunneling of the hydrogen atom drastically as seen in the present calculations.

V. CONCLUSION

The MP2(fc)/6-311G(3df,3pd) calculations were employed to construct a potential energy surface for the abstraction reaction $\text{H}_2\text{S} + \text{O}(^3\text{P}) \rightarrow \text{SH} + \text{OH}$. Quantum mechanical reactive scattering calculations were performed under an assumption of atom-diatom collinear collisions. It was found that the rate constant was drastically enhanced in comparison with the result of simple transition-state theory calculations, suggesting that tunneling should play an important role in the abstraction reaction at room temperature.

- ¹D. L. Singleton, G. Paraskevopoulos, and R. S. Irwin, *J. Phys. Chem.* **86**, 2605 (1982).
- ²F. E. Davidson, A. R. Clemo, G. L. Duncan, R. J. Browett, J. H. Hobson, and R. Grice, *Mol. Phys.* **46**, 33 (1982).
- ³A. R. Clemo, F. E. Davidson, G. L. Duncan, and R. Grice, *Chem. Phys. Lett.* **84**, 509 (1981).
- ⁴N. Balucani, L. Beneventi, P. Casavecchia, D. Stranges, and G. G. Volpi, *J. Chem. Phys.* **94**, 8611 (1991).
- ⁵I. R. Slagle, F. Balocchi, and D. Gutman, *J. Phys. Chem.* **82**, 1333 (1978).
- ⁶D. A. Whytock, R. B. Timmons, J. H. Lee, J. V. Michael, W. A. Payne, and L. J. Stief, *J. Chem. Phys.* **65**, 2052 (1976).
- ⁷D. L. Singleton, R. S. Irwin, W. S. Nip, and R. J. Cvetanovic', *J. Phys. Chem.* **83**, 2195 (1979).
- ⁸K. Tsuchiya, K. Yokoyama, H. Matsui, M. Oya, and G. Dupre, *J. Phys. Chem.* **98**, 8419 (1994).
- ⁹S. Takane and T. Fueno, *Bull. Chem. Soc. Jpn.* **66**, 3633 (1993).
- ¹⁰Z. Z. Zhu, J. J. W. McDouall, D. J. Smith, and R. Grice, *Chem. Phys. Lett.* **188**, 520 (1992).
- ¹¹A. Goumri, D. Laakso, J.-D. R. Rocha, C. E. Smith, and P. Marshall, *J. Chem. Phys.* **102**, 161 (1995).
- ¹²M. F. R. Mulcahy, *Gas Kinetics* (Nelson, London, 1973).
- ¹³J. N. L. Connor, *Comput. Phys. Commun.* **17**, 117 (1979).
- ¹⁴*The Theory of Chemical Reaction Dynamics*, edited by D. C. Clary (Reidel, Dordrecht, 1986).
- ¹⁵F. Webster and J. C. Light, *J. Chem. Phys.* **90**, 265 (1989).
- ¹⁶G. Nyman and D. C. Clary, *J. Chem. Phys.* **100**, 3556 (1994).
- ¹⁷D. C. Clary, *J. Chem. Phys.* **95**, 7298 (1991).
- ¹⁸J. M. Bowman, *J. Phys. Chem.* **95**, 4960 (1991).
- ¹⁹D. H. Zhang and J. Z. H. Zhang, *J. Chem. Phys.* **99**, 5615 (1993).
- ²⁰U. Manthe, T. Seideman, and W. H. Miller, *J. Chem. Phys.* **99**, 10078 (1993).
- ²¹D. Neuhauser, *J. Chem. Phys.* **100**, 9272 (1994).
- ²²N. Balakrishnan and G. D. Billing, *J. Chem. Phys.* **101**, 2785 (1994).
- ²³H. Szichman, A. J. C. Varandas, and M. Baer, *J. Chem. Phys.* **102**, 3474 (1995).
- ²⁴J. M. Bowman and G. C. Schatz, *Annu. Rev. Phys. Chem.* **46**, (1995).
- ²⁵T. Takayanagi, *Bull. Chem. Soc. Jpn.* **68**, 2527 (1995).
- ²⁶T. H. Dunning, Jr. and P. J. Hay, *Methods of Electronic Structure Theory*, edited by H. R. Shaefer III (Plenum, New York, 1977), p. 1.
- ²⁷GAUSSIAN 90, M. J. Frisch, M. Head-Gordon, G. W. Trucks, J. B. Foresman, H. B. Schlegel, K. Raghavachari, M. A. Robb, J. S. Binkley, C. Gonzalez, D. J. DeFrees, D. J. Fox, R. A. Whiteside, R. Seeger, C. F. Melius, J. Baker, R. L. Martin, R. L. Kahn, J. J. P. Stewart, S. Topiol, and J. A. Pople (Gaussian Inc., Pittsburgh, PA, 1990).
- ²⁸R. T. Pack, *J. Chem. Phys.* **60**, 633 (1974).
- ²⁹J. C. Light and R. B. Walker, *J. Chem. Phys.* **65**, 4272 (1976).
- ³⁰D. Wang and J. M. Bowman, *J. Chem. Phys.* **98**, 6235 (1990).
- ³¹H. B. Schlegel, *J. Phys. Chem.* **92**, 3073 (1988).
- ³²K. Yamaguchi, Y. Takahara, T. Fueno, and K. N. Houk, *Theor. Chim. Acta* **73**, 337 (1988).
- ³³E. Pollak, M. S. Child, and P. Pechukas, *J. Chem. Phys.* **72**, 1669 (1980).
- ³⁴S.-F. Wu, B. R. Johnson, and R. D. Levine, *Mol. Phys.* **25**, 839 (1973).